



Measurement report: Method for evaluating CO₂ emission from a cement plant by atmosphere O₂/N₂ and CO₂ measurements and its applicability to the detection of CO₂ capture signals

Shigeyuki Ishidoya¹, Kazuhiro Tsuboi², Hiroaki Kondo¹, Kentaro Ishijima², Nobuyuki Aoki¹, Hidekazu Matsueda², and Kazuyuki Saito³

¹National Institute of Advanced Industrial Science and Technology (AIST), Tsukuba 305-8569, Japan,

²Meteorological Research Institute, Tsukuba, Japan, Tsukuba305-0052, Japan,

³Japan Meteorological Agency, Tokyo, Japan, Tokyo 105-8431, Japan

Correspondence to: Shigeyuki Ishidoya (s-ishidoya@aist.go.jp)

Abstract. Continuous observations of the atmospheric O₂/N₂ ratio and CO₂ amount fractions have been carried out at Ryori (RYO), Japan since August 2017. In these observations, the O₂:CO₂ exchange ratio (oxidative ratio (OR), $-\Delta y(\text{O}_2)\Delta y(\text{CO}_2)^{-1}$) has frequently been lower than expected from short-term variations in emissions from terrestrial biospheric activities and combustion of liquid, gas, and solid fuels. This finding suggests a significant effect of CO₂ emission from a cement plant located about 6 km northwest of RYO. To evaluate this effect quantitatively, we simulated CO₂ amount fractions in the area around RYO by using a fine-scale atmospheric transport model that incorporated CO₂ fluxes from terrestrial biospheric activities, fossil fuel combustion, and cement production. The simulated CO₂ amount fractions were converted to O₂ amount fractions by using the respective OR values for each of the incorporated CO₂ fluxes, and then simulated OR values were calculated from the calculated O₂ and CO₂ amount fractions. To extract the contribution of CO₂ emissions from the cement plant, we used $y(\text{CO}_2^*)$ as an indicator variable, where $y(\text{CO}_2^*)$ is a conservative variable for terrestrial biospheric activity and fossil fuel combustion obtained by simultaneous analyses of observed O₂/N₂ ratios and CO₂ amount fractions and simulated ORs. We confirmed that the observed and simulated OR values and also the $y(\text{CO}_2^*)$ values and simulated CO₂ amount fractions due only to cement production were generally consistent. These results suggest that combined measurements of O₂/N₂ ratios and CO₂ amount fractions will be useful for evaluating CO₂ capture from flue gas at carbon capture and storage (CCS) plants, which, similar to a cement plant, change CO₂ amount fractions without changing O₂ values, although CCS plants differ from cement plants in the direction of CO₂ exchange with the atmosphere.

1 Introduction

Simultaneous analyses of atmospheric O₂/N₂ ratios and CO₂ amount fractions have been used to estimate the global CO₂ budget since the early 1990s (e.g. Keeling and Shertz, 1992). Recently, these analyses have also been applied to separate the contributions of different sources to the local CO₂ budget in an urban area (Ishidoya et al., 2020; Sugawara et al., 2021). This approach uses $-\text{O}_2:\text{CO}_2$ exchange ratios (i.e. the oxidative ratio (OR), $-\Delta y(\text{O}_2)\Delta y(\text{CO}_2)^{-1}$) for terrestrial biospheric activities



and fossil fuel combustion. For terrestrial biospheric O₂ and CO₂ fluxes, ORs of 1.1 or 1.05 are generally used (Severinghaus, 1995; Resplandy et al., 2019), and for the fluxes due to fossil fuel combustion, ORs of 1.95 for gaseous fuels, 1.44 for oil and other liquid fuels, 1.17 for coal and other solid fuels, and 0 for cement production are typical (Keeling, 1988). Therefore, atmospheric O₂ and CO₂ fluxes due to terrestrial biospheric activities and fossil fuel combustion (excluding cement production) vary in opposite phase.

In the cement production process, calcium carbonate is burned and calcium oxide and CO₂ are produced as follows:



40

Because this chemical reaction emits CO₂ to the atmosphere without O₂ consumption, its OR is 0. It should be noted that the cement kilns are usually fired with fossil fuels, so that the overall OR for cement production is not 0. CO₂ emissions from cement production account for about 4 % of global fossil CO₂ emissions (Friedlingstein et al., 2020), and this value is included in global CO₂ budget analyses based on the atmospheric O₂/N₂ ratio (e.g. Manning and Keeling, 2006). However, because it is difficult to separate the cement production signal from CO₂ emissions due to fossil fuel combustion and terrestrial biospheric activities, no study has reported direct evidence of variations in the atmospheric CO₂ amount fraction due to cement production at the Global Atmosphere Watch (GAW) program of the World Meteorological Organization (WMO) stations. In this context, simultaneous observations of O₂/N₂ ratios and CO₂ amount fractions are expected to be useful for separating out the cement production signal owing to its characteristic OR value. Moreover, Keeling et al. (2011), who examined the possibility of verifying rates of carbon capture and storage (CCS) and direct air capture of CO₂ (DAC) by using changes in the atmospheric constituents, suggested that combined measurements of the O₂/N₂ ratio and CO₂ could powerfully constrain estimated rates.

To investigate CO₂ leak detection from a CCS site, Leeuwen and Meijer (2015) observed O₂/N₂ ratios and CO₂ from a 6-m-tall mast that was 5–15 m away from artificial CO₂ release points. They estimated that their measurement system could detect a CO₂ leak of 10³ t a⁻¹ at a location up to 500 m away from the leak point. Pak et al. (2016) monitored the air for CO₂ plumes at locations between 1 and 100 m from an artificial CO₂ release point, and collected air samples typically between 9 and 20 m from the point where the CO₂ amount fraction was 100–600 μmol mol⁻¹ above ambient. They then analyzed the air samples for O₂ and CO₂ amount fractions and found much lower ORs than those expected from fossil fuel combustion and terrestrial biospheric activities. These studies support the suggestion by Keeling et al. (2011) regarding the usefulness of O₂/N₂ ratios and CO₂ measurements. As the next step to verify the usefulness of combined measurements of O₂/N₂ ratios and CO₂, their applicability to the detection of not only CO₂ leaks but also CO₂ capture from flue gas should be examined. In this regard, CCS/DAC plants remove CO₂ from the atmosphere without causing any O₂ changes, just as cement plants do, differing only in the direction of CO₂ exchange between the plant and the atmosphere. Therefore, it should be possible to evaluate the ability of combined measurements to detect a CO₂ capture signal by showing that they can be used to detect a cement production signal.

55
60



65 In this paper, we present evidence of the successful detection of a cement production signal by combined measurements of O₂/N₂ ratios and CO₂ at a ground station (a designated WMO/GAW local site) located near a cement plant. We also examine the usefulness of the measurements for future detection of CCS/DAC signals by using a fine-scale 3-D atmospheric transport model to investigate the consistency between the observed signal and the simulated CO₂ emissions from the plant.

2 Methods

70 Atmospheric O₂/N₂ ratios and CO₂ amount fractions have been observed continuously at Ryori (RYO: 39° 2' N, 141° 49' E; Fig. 1), Japan, since 2017, by using a paramagnetic O₂ analyzer (POM-6E, Japan Air Liquid) and a non-dispersive infrared CO₂ analyzer (NDIR; LI-7000, LI-COR), respectively. RYO is a designated WMO/GAW station, and the Japan Meteorological Agency (JMA) has also observed CO₂, CH₄, and CO amount fractions there since 1987, 1991, and 1991, respectively (e.g. Wada et al., 2011). The CO₂, CH₄, and CO amount fraction data observed by JMA are available online at
75 the WMO World Data Centre for Greenhouse Gases (WMO/WDCGG; <https://gaw.kishou.go.jp/>). A cement plant (Taiheiyo Cement Ofunato plant) is 6 km away from RYO (Fig. 1). It should be noted that the CO₂ amount fraction data posted on WDCGG have already been classified into the data for background air and those affected by local fossil fuel combustion including the cement production discussed in this study. The annual cement production at the plant is 1.966 × 10⁶ t a⁻¹ (<https://www.taiheiyo-cement.co.jp/english/index.html>).

80 The O₂/N₂ ratio is reported as δ(O₂/N₂) in per meg, where 1 per meg is 0.001 ‰:

$$\delta(\text{O}_2/\text{N}_2) = \frac{R_{\text{sample}}(^{16}\text{O}^{16}\text{O}/^{14}\text{N}^{14}\text{N})}{R_{\text{standard}}(^{16}\text{O}^{16}\text{O}/^{14}\text{N}^{14}\text{N})} - 1, \quad (2)$$

where the subscripts “sample” and “standard” indicate the sample air and the standard gas, respectively. Because O₂ amount
85 fraction in dry air is 0.2093 to 0.2094 mol mol⁻¹ (Tohjima et al., 2005; Aoki et al., 2019), the addition of 1 μmol of O₂ to 1 mol of dry air increases δ(O₂/N₂) by 4.8 per meg (= 1/0.2094). If CO₂ is converted one-for-one into O₂, it causes δ(O₂/N₂) to increase by 4.8 per meg, which is equivalent to an increase of 1 μmol mol⁻¹ of O₂ for each 1 μmol mol⁻¹ decrease in CO₂. Therefore, observed relative changes in δ(O₂/N₂) were converted to those in O₂ amount fraction by dividing by the ratio 4.8 per meg (μmol mol⁻¹)⁻¹.

90 In this study, δ(O₂/N₂) of each air sample was measured with a paramagnetic analyzer using working standard air that had been measured against our primary standard air (Cylinder No. CRC00045; AIST-scale) using a mass spectrometer (Thermo Scientific Delta-V) (Ishidoya and Murayama, 2014). The dilution effects on the O₂ amount fraction measured by the paramagnetic analyzer were corrected experimentally, not only for the changes in the CO₂ of the sample air or standard gas measured by the NDIR but also for the changes in the Ar amount fraction of the standard gas measured by the mass
95 spectrometer as δ(Ar/N₂). The analytical reproducibility of the δ(O₂/N₂) and CO₂ amount fraction measurements by the system



was about 5 per meg and $0.06 \mu\text{mol mol}^{-1}$, respectively, for 2-minute-average values. Details of the continuous measurement system used are given in Ishidoya et al. (2017). Note that we used a mass spectrometer to measure both $\delta(\text{O}_2/\text{N}_2)$ and the CO_2 amount fraction of the working standard air, whereas we determined the CO_2 amount fraction on the TU-10 scale using a gravimetrically prepared air-based CO_2 standard gas system (Nakazawa et al., 1997). However, we found that the CO_2 amount fractions observed in this study were systematically higher by about $1 \mu\text{mol mol}^{-1}$ than those observed by JMA and reported on the WMO scale, which is larger than that expected from the scale difference of about $0.2 \mu\text{mol mol}^{-1}$ between the TU-10 and WMO scales (Tsuboi et al., 2016). This discrepancy might be related to the LI-7000 NDIR used in this study because no significant difference has been found between the TU-10 and WMO scales at Minamitorishima, where a different NDIR (LI-820, LI-COR) has been used for continuous measurements of $\delta(\text{O}_2/\text{N}_2)$ and CO_2 amount fractions (Ishidoya et al., 2017). However, we found no significant difference in span sensitivities between the CO_2 amount fractions observed in this study and those observed by JMA. Therefore, the systematic difference between the observed CO_2 amount fractions and those observed by JMA does not affect the OR values, discussed in section 3, which were calculated from changes in O_2 and CO_2 amount fractions.

To calculate local transport of CO_2 around RYO, we used the National Institute of Advanced Industrial Science and Technology (AIST) Mesoscale Model (AIST-MM) fine-scale regional atmospheric transport model (Kondo et al., 2001). AIST-MM is a one-way nested model with an outer domain that covers East Japan with an approximately 10-km grid interval and an inner domain that covers an area of 120 km by 120 km near Ryori with a grid interval of approximately 1 km. The EAGrid2010-Japan emissions inventory (Fukui et al., 2014), an update of the EAGrid2000-Japan inventory (Kannari et al., 2007) to the year 2010, was used for anthropogenic CO_2 sources. Spatial resolution of EAGrid2010-Japan is approximately 1 km, and temporal resolution is monthly average of 1 hour. No further inter-annual correction of emissions is employed, but EAGrid2010-Japan considers the difference in traffic volume between weekdays and holidays. To calculate the CO_2 budget for vegetation, the NCAR Land Surface Model (Bonan, 1996) was used as a sub-model, replacing the simple function of temperature and solar insolation used in the original AIST-MM for this calculation. The cement plant source was set at the location of the plant's stack, at the effective stack height of 275 m. The CO_2 emissions from the cement plant were estimated from the clinker production capacity of the Ofunato plant in 2018 (Japan Cement Association 2020). The annual emission was calculated using the method of the Ministry of Environmental Protection (https://www.env.go.jp/earth/ondanka/ghg-mrv/methodology/material/methodology_2A1.pdf, in Japanese) as

$$E = P \times F \times D, \quad (3)$$

where E is the annual emission of CO_2 from the cement plant (t a^{-1}), P is the annual production capacity of clinker at the cement plant (t a^{-1}), F is the CO_2 -to-clinker mass ratio of 0.516, and D is the cement kiln dust of 1. For initial and boundary conditions, we used GPV/MSM (grid point value of meso-scale model) meteorological data of wind, temperature, and humidity from JMA (<https://www.jma.go.jp/jma/en/Activities/nwp.html>).



3 Results and discussion

From August 2017 to November 2018, $\delta(O_2/N_2)$ and CO_2 amount fractions observed at RYO varied cyclically in opposite
130 phase to each other on timescales from several hours to seasonal (Fig. 2); however, variations in CO_2 and CO amount fractions
were roughly in phase. The opposite-phase variations of $\delta(O_2/N_2)$ and CO_2 amount fractions were driven by fossil fuel
combustion and terrestrial biospheric activities. In contrast, the atmospheric O_2 variation ($\mu\text{mol mol}^{-1}$) due to the air–sea
exchange of O_2 is much larger than that of CO_2 on timescales shorter than 1 year because of the difference in their equilibration
times between the atmosphere and the surface ocean: the equilibration time for O_2 is much shorter than that for CO_2 because
135 of the carbonate dissociation effect on the air–sea exchange of CO_2 (Keeling et al., 1993). The in-phase variations of the CO_2
and CO amount fractions were also driven by fossil fuel combustion and biomass burning. CO:CO₂ ratios for fossil fuel
combustion and biomass burning reported by past studies are about 0.01–0.04 and >0.1, respectively (e.g. Nara et al., 2011;
Tohjima et al., 2014; Niwa et al., 2014). The short-term (several hours to several days) variations in CO:CO₂ ratios were about
0.01 from late autumn to early spring, but they were much smaller in summer (Fig. 2). These results suggest, therefore, that
140 the short-term variations in $\delta(O_2/N_2)$ and CO_2 amount fractions were driven mainly by fossil fuel combustion in winter and
mainly by terrestrial biospheric activities in summer. CO amount fractions also showed a seasonal cycle with a summertime
minimum that is attributed to the air mass around Japan: in winter the air mass is of continental origin and in summer it is of
maritime origin.

In this study, we focused on the short-term variations in $\delta(O_2/N_2)$ and the CO_2 and CO amount fractions (Fig. 2).
145 Therefore, we subtracted 1-week average values of $\delta(O_2/N_2)$ and the CO_2 and CO amount fractions from the observed values,
and examined the relationships among the residuals ($\Delta y(O_2)$, $\Delta y(CO_2)$, and $\Delta y(CO)$; Fig. 3). Here, $\Delta y(O_2)$ is the equivalent
value in $\mu\text{mol mol}^{-1}$ converted from $\delta(O_2/N_2)$. Many of the $\Delta y(O_2)$ and $\Delta y(CO_2)$ values show the expected relationship with
the OR for a composite flux from terrestrial biospheric activities and the consumption of gas, liquid, and solid fuels, similar to
values observed at other Japanese sites (e.g. Minejima et al., 2012; Goto et al., 2013; Ishidoya et al., 2020). Moreover, it is
150 clear that relationships with an OR smaller than 1.1 appear frequently, especially for data with high $\Delta y(CO)$ values. Although
these characteristic relationships have previously been observed only in artificial CO_2 release experiments such as those
described by Leeuwen and Meijer (2015) and Pak et al. (2016), they can be interpreted as indicating a significant CO_2 flux
from cement production, which has an OR value of 0. Therefore, we used the AIST-MM model to calculate atmospheric CO_2
amount fractions, with or without taking into account the CO_2 flux from the cement plant near RYO, and to convert the
155 calculated CO_2 amount fractions to O_2 amount fractions using the respective OR values of fossil fuels and terrestrial biospheric
activities. Then we compared the observed and simulated OR values.

In October 2017, short-term variations in observed CO_2 and $\delta(O_2/N_2)$ were opposite in phase, and the amplitudes (in
 $\mu\text{mol mol}^{-1}$) of some CO_2 variations were larger than those of the corresponding $\delta(O_2/N_2)$ variations (Fig. 4a). This result
suggests an effect of cement production. Similar characteristic variations suggesting a cement production effect were also seen
160 in the observations made at RYO in November 2017 and in February, May, and August 2018 (Fig. 4b–e). The simulated CO_2



amount fraction, calculated from the sources and sinks in East Japan area with no background amount fraction by the AIST-MM, is also shown in Fig. 4. Comparison between the observed and simulated CO₂ amount fractions showed weak correlations: correlation coefficients were 0.41, 0.28, 0.19, 0.33, and 0.54 for October and November 2017 and February, May, and August, 2018, respectively. Therefore, the AIST-MM reproduced the general characteristics of the observed short-term variations in
165 CO₂, but not necessarily the phase and amplitude of individual variations. The discrepancies between observed and simulated values can be attributed to the limited resolution of the model, or to problems in the parameterization of transport processes, or in the CO₂ sources/sinks incorporated into the AIST-MM.

The contribution of CO₂ amount fraction for the three components (cement production, land biospheric activities, and fossil fuel consumption other than cement production) are also shown in Fig. 4. The results demonstrate that cement production
170 contributed significantly to the simulated CO₂ amount fraction. We examined the effect of cement production on OR values by calculating OR values by fitting regression lines to the observed and simulated O₂ and CO₂ amount fractions during successive 24-h periods (Fig. 4, bottom). For this purpose, we converted the simulated CO₂ amount fractions to O₂ amount fractions by assuming OR values of 0, 1.1, and 1.4 for cement production, terrestrial biospheric activities, and fossil fuel combustion, respectively. For comparison, we also calculated OR values for the O₂ and CO₂ amount fractions simulated
175 without considering the contribution of cement production. Both the observed OR values and those simulated considering cement production are frequently lower than 1.1, but no OR values simulated without considering cement production are lower than 1.1. Therefore, CO₂ emissions from the cement plant must be incorporated into the transport model to reproduce the detailed variations in atmospheric O₂ and CO₂ amount fractions at RYO.

Next, we extracted signals of cement production based on the simultaneous measurements of $\delta(\text{O}_2/\text{N}_2)$ and CO₂ amount
180 fractions. For this purpose, we use $y(\text{CO}_2^*)$ as an indicator:

$$y(\text{CO}_2^*) = \Delta y(\text{CO}_2) + \frac{X(\text{O}_2)}{\alpha_{B+F}} \Delta \delta(\text{O}_2/\text{N}_2), \quad (4)$$

where $\Delta y(\text{CO}_2)$ and $\Delta \delta(\text{O}_2/\text{N}_2)$ are the deviations of the observed CO₂ amount fractions and $\delta(\text{O}_2/\text{N}_2)$, respectively, from their monthly mean values, $X(\text{O}_2)$ ($= 0.2094$) is the fraction of atmospheric O₂, and α_{B+F} is the expected OR for terrestrial biospheric activities and fossil fuel combustion. The $y(\text{CO}_2^*)$ is closely related to atmospheric potential oxygen ($\delta(\text{APO})$), which is
185 conserved for terrestrial biospheric activities (Stephens et al., 1998). In our previous study, we calculated $\delta(\text{APO})$ as:

$$\delta(\text{APO}) = \delta(\text{O}_2/\text{N}_2) + \frac{\alpha_B}{X(\text{O}_2)} y(\text{CO}_2) - 2000 \times 10^{-6}, \quad (5)$$

where 2000 is an arbitrary reference (Ishidoya et al., 2022). For α_{B+F} values, we used monthly average OR values calculated from the simulated O₂ and CO₂ values without considering the contribution of cement production (Fig. 4, bottom). If there are no significant contributions from air–sea O₂ and CO₂ exchanges, then $y(\text{CO}_2^*)$ indicates the change in the atmospheric CO₂
190 amount fraction due only to cement production. No air–sea exchanges can be assumed if the wind field and surface ocean biological production are constant throughout the month; however, past studies have reported that $\delta(\text{O}_2/\text{N}_2)$ shows day-to-day variation due to the air–sea O₂ exchange and its atmospheric transport (e.g. Goto et al., 2017). However, changes in CO₂ amount fractions observed when the OR was lower than 1.1 occurred over periods of less than a day (Fig. 4a–e).



195 Taking these findings into consideration, we derived the baseline variation in $y(\text{CO}_2^*)$, which does not include a significant contribution from cement production, as follows. First, we calculated the standard deviation (1σ) of each $y(\text{CO}_2^*)$ value from the 24-h running means of $y(\text{CO}_2^*)$. Then, we removed $y(\text{CO}_2^*)$ values greater than the 24-h running mean of $y(\text{CO}_2^*) + 1\sigma$ from the analyses. Finally, we recalculated the 24-h running means by using the residual $y(\text{CO}_2^*)$ values, and regarded them as the baseline variation. Accordingly, the $y(\text{CO}_2^*)$ anomaly obtained by subtracting the baseline variation from each $y(\text{CO}_2^*)$ value is considered to indicate CO_2 changes due only to the contribution of the cement production.

200 In October 2017, $y(\text{CO}_2^*)$ and CO amount fraction maxima at RYO appeared at the same time that the wind was blowing from the northwest (most frequently over the range of $270\text{--}300^\circ$) (https://www.data.jma.go.jp/env/data/report/data/download/atm_bg_e.html) (Fig. 5a). This result suggests that the short-term variations in $y(\text{CO}_2^*)$ were driven mainly by air masses transported from the cement plant, which is about 6 km northwest of RYO. These findings also indicate that it is possible to extract CO_2 amount fraction data from background air at RYO by
205 selecting observed OR and CO amount fraction data. We have confirmed the present method of JMA used to select background air for the data posted on WDCGG is sufficient to exclude the effect of cement production, nevertheless the use of OR may provide an additional constraint. Note that CO is emitted during fossil fuel combustion at the cement plant to supply electricity and heat for cement production. This means CO_2 presumably as well, and the overall OR of cement production would not be 0.

210 To examine the consistency between the observed $y(\text{CO}_2^*)$ and simulated CO_2 emissions from the cement plant, we compared 5-h means of $y(\text{CO}_2^*)$ anomalies with changes in the CO_2 amount fraction due to the contribution of cement production as simulated by the AIST-MM (hereafter referred to as “ $y(\text{CO}_2, \text{cement})$ ”) (Fig. 5a, bottom). The result shows that variations in the $y(\text{CO}_2^*)$ anomaly and $\text{CO}_{2\text{cement}}$ are of the same order of magnitude, although they do not necessarily occur simultaneously. This result suggests that we succeeded in using $y(\text{CO}_2^*)$ to detect a signal of CO_2 emission from the cement
215 plant, and that this signal can be used to validate a fine-scale atmospheric transport model. In this context, Leeuwen and Meijer (2015) suggested that a CO_2 leak of 10^3 t a^{-1} is detectable at a location up to 500 m away from the leak point based on their observations of atmospheric O_2 and CO_2 amount fractions. If this relationship follows an inverse square law, a CO_2 leak of $1.44 \times 10^5 \text{ t a}^{-1}$ should be detectable at locations up to 6 km from the leak point. Therefore, about 10^6 t a^{-1} of the CO_2 emission from the cement plant in this study, calculated with Eq. (3), is large enough to be detected at RYO. Features during November
220 2017 and May and August 2018 were similar (Fig. 5b, d, e), although the short-term variations in $y(\text{CO}_2^*)$ in May 2018 (Fig. 5d) were noisier than in the other months, probably because of an effect of short-term variations in the air–sea O_2 flux due to high primary production during the spring bloom in the nearby coastal ocean (e.g. Yamagishi et al., 2008). In February 2018, however, the monthly mean $y(\text{CO}_2^*)$ anomaly was around zero (Fig. 5c), whereas $y(\text{CO}_2, \text{cement})$ was notably higher.

225 The monthly mean $y(\text{CO}_2^*)$ anomalies shown in Fig. 5a–e were calculated using the OR (α_{B+F}) value calculated by the AIST-MM for terrestrial biospheric activities and fossil fuel consumption excluding cement production. In Fig. 6, these $y(\text{CO}_2^*)$ anomaly values as well as those calculated using α_{B+F} values of 1.4 and 1.1 are compared with monthly mean $y(\text{CO}_2,$



cement) values. The monthly mean $\gamma(\text{CO}_2^*)$ anomalies were lower during autumn and winter and higher during spring and summer than the monthly mean $\gamma(\text{CO}_2, \text{cement})$ values. We have confirmed monthly mean $\gamma(\text{CO}_2, \text{cement})$ values were related to the occurrence of northwesterly winds (i.e. wind blowing from the cement plant). Moreover, the production of clinker at the cement plant in February 2018, when a discrepancy was observed between the $\gamma(\text{CO}_2^*)$ anomalies and $\gamma(\text{CO}_2, \text{cement})$, was not markedly different from the production in the other months (personal communication with Taiheiyo Cement Co.). Therefore, the discrepancy between the monthly mean $\gamma(\text{CO}_2^*)$ anomaly and $\gamma(\text{CO}_2, \text{cement})$ in February 2018 may be related to inadequate representation of the local transport of CO_2 by the AIST-MM due to the complicated geography around RYO. Moreover, except in February 2018, the monthly mean $\gamma(\text{CO}_2^*)$ anomaly did not depend on the α_{B+F} value used to calculate $\gamma(\text{CO}_2^*)$ (Fig. 6). In addition, the average monthly mean $\gamma(\text{CO}_2^*)$ anomaly values and the average $\gamma(\text{CO}_2, \text{cement})$ during the 5 months (right side of Fig. 6) agreed within their monthly variabilities. These results suggest that it is not necessary to use the α_{B+F} value simulated by the AIST-MM to estimate the contribution of cement production to the atmospheric CO_2 amount fraction at RYO; rather, it can be estimated from only the observed $\gamma(\text{CO}_2^*)$ by assuming an α_{B+F} value of 1.1 or 1.4. Therefore, the observed $\gamma(\text{CO}_2^*)$ can be used to validate monthly to annual average CO_2 fluxes from cement production simulated by a fine-scale atmospheric transport model.

$\gamma(\text{CO}_2^*)$ is expected to be an indicator for detecting the signal of CO_2 capture from the flue gas at the cement plant. At a cement plant, CO_2 is removed from the flue gas without any O_2 changes. Therefore, if the CO_2 emitted during cement production, which is about 10^6 t a^{-1} at this plant, is removed from the flue gas, then the 5-month mean $\gamma(\text{CO}_2^*)$ anomaly would change from 0.4 to $0 \mu\text{mol mol}^{-1}$. Thus, a cement plant can be a useful site not only for demonstrating carbon capture from flue gas but also for monitoring its efficiency based on combined measurements of $\delta(\text{O}_2/\text{N}_2)$ and CO_2 . In addition, during the future operation of a large-scale DAC plant, a negative annual mean $\gamma(\text{CO}_2^*)$ anomaly value should be observed because a DAC plant removes CO_2 from the atmosphere without emitting O_2 to the atmosphere.

4 Summary

We analyzed atmospheric $\delta(\text{O}_2/\text{N}_2)$ and CO_2 and CO amount fraction data observed continuously at RYO to extract a CO_2 emission signal from a cement plant located about 6 km northwest of RYO. The observed $\delta(\text{O}_2/\text{N}_2)$ and CO_2 amount fractions varied cyclically in opposite phase to each other on timescales from several hours to seasonal. From the $\text{CO}:\text{CO}_2$ ratios, the short-term variations in $\delta(\text{O}_2/\text{N}_2)$ and CO_2 amount fraction were inferred to be driven mainly by fossil fuel combustion in winter and by terrestrial biospheric activities in summer. We found that an OR lower than 1.1 was frequently associated with short-term variations, especially when the CO amount fraction was high; this result suggests a significant effect of cement production, which has an OR of 0. We compared observed CO_2 amount fractions with those simulated by the AIST-MM for October and November 2017 and February, May, and August 2018. The general characteristics of the short-term variations in the observed CO_2 amount fraction were reproduced by the AIST-MM, although not necessarily their phases or



amplitudes. We calculated the simulated OR values by using simulated $\delta(O_2/N_2)$ values obtained from simulated CO_2 amount fractions and OR values of 1.1, 1.4, and 0 for terrestrial biospheric activities, fossil fuel combustion, and cement production, respectively. As in the observations, simulated OR values lower than 1.1 were frequently associated with short-term variations. $y(CO_2^*)$ was calculated from the observed $\delta(O_2/N_2)$ and CO_2 amount fractions and the simulated α_{B+F} to extract the cement production signal. Variations in the $y(CO_2^*)$ anomaly relative to baseline values were generally of the same order of magnitude as CO_2 amount fraction changes due to contribution of cement production simulated by the AIST-MM ($y(CO_2, \text{cement})$). The monthly mean $y(CO_2^*)$ anomaly averaged over the 5 months examined in this study and the 5-month average of $y(CO_2, \text{cement})$ agreed within their variabilities. These results confirm that monthly to annual average CO_2 emissions from a cement plant can be detected by using $y(CO_2^*)$, and, therefore, that a cement plant will be a useful site for demonstrating and monitoring CO_2 capture from flue gas in the future.

Data availability.

The $\delta(O_2/N_2)$ and CO_2 amount fraction data at RYO site presented in this study are included as electronic supplement to the manuscript. We will deposit the data in an appropriate data archive before the manuscript is accepted for publication.

Author contributions.

SI designed the study and drafted the manuscript. Measurements of O_2 and CO_2 amount fractions were conducted by SI, KT, and KS. KH conducted the AIST-MM simulations. NA prepared the standard gas for the O_2 measurements. KI and HM examined the results and provided feedback on the manuscript. All authors approved the final manuscript.

Competing interests.

The authors declare that they have no conflict of interest.

280

Acknowledgements.

We acknowledge the many staff members of the Japan Meteorological Agency. We also thank Shohei Murayama at the National Institute of Advanced Industrial Science and Technology (AIST), Ryo Fujita at the Meteorological Research Institute, and JANS Co. Ltd. for supporting the observation.

285

Financial support.

This study was partly supported by JSPS KAKENHI (grant nos. 19H01975 and 22H05006) and the Global Environment Research Coordination System from the Ministry of the Environment, Japan (grant nos. METI1454 and METI1953).



290 References

- Aoki, N., Ishidoya, S., Matsumoto, N., Watanabe, T., Shimosaka, T., and Murayama, S.: Preparation of primary standard mixtures for atmospheric oxygen measurements with less than 1 $\mu\text{mol mol}^{-1}$ uncertainty for oxygen molar fractions, *Atmos. Meas. Tech.*, 12, 2631–2646, <https://doi.org/10.5194/amt-12-2631-2019>, 2019.
- Bonan, G. B.: A Land surface model (LSM version 1.0) for ecological, hydrological, and atmospheric studies: Technical description and user's guide, Climate and global dynamics division, National Center for Atmospheric Research, Boulder, Colorado, 150 pp., 1996.
- Friedlingstein, P., O'Sullivan, M., Jones, M. W., Andrew, R. M., Hauck, J., Olsen, A., Peters, G. P., Peters, W., Pongratz, J., Sitch, S., Le Quéré, C., Canadell, J. G., Ciais, P., Jackson, R. B., Alin, S., Aragão, L. E. O. C., Arneeth, A., Arora, V., Bates, N. R., Becker, M., Benoit-Cattin, A., Bittig, H. C., Bopp, L., Bultan, S., Chandra, N., Chevallier, F., Chini, L. P., Evans, W., Florentie, L., Forster, P. M., Gasser, T., Gehlen, M., Gilfillan, D., Gkritzalis, T., Gregor, L., Gruber, N., Harris, I., Hartung, K., Haverd, V., Houghton, R. A., Ilyina, T., Jain, A. K., Joetzjer, E., Kadono, K., Kato, E., Kitidis, V., Korsbakken, J. I., Landschützer, P., Lefèvre, N., Lenton, A., Lienert, S., Liu, Z., Lombardozzi, D., Marland, G., Metzl, N., Munro, D. R., Nabel, J. E. M. S., Nakaoka, S.-I., Niwa, Y., O'Brien, K., Ono, T., Palmer, P. I., Pierrot, D., Poulter, B., Resplandy, L., Robertson, E., Rödenbeck, C., Schwinger, J., Séférian, R., Skjelvan, I., Smith, A. J. P., Sutton, A. J., Tanhua, T., Tans, P. P., Tian, H., Tilbrook, B., van der Werf, G., Vuichard, N., Walker, A. P., Wanninkhof, R., Watson, A. J., Willis, D., Wiltshire, A. J., Yuan, W., Yue, X., and Zaehle, S.: Global Carbon Budget 2020, *Earth Syst. Sci. Data*, 12, 3269–3340, <https://doi.org/10.5194/essd-12-3269-2020>, 2020.
- Fukui, T., Kokuryo, K., Baba, T., Kannari, A.: Updating EAGrid2000-Japan emissions inventory based on the recent emission trends, *J. Jpn. Soc. Atmos. Environ.* 49 (2), 117–125, 2014 (in Japanese).
- Goto, D., Morimoto, S., Ishidoya, S., Ogi, A., Aoki, S., and Nakazawa, T.: Development of a high precision continuous measurement system for the atmospheric O_2/N_2 ratio and its application at Aobayama, Sendai, Japan, *J. Meteorol. Soc. Jpn.*, 91, 179–192, 2013.
- Goto, D., Morimoto, S., Aoki, S., Patra, P. K., and Nakazawa, T.: Seasonal and short-term variations in atmospheric potential oxygen at Ny-Ålesund, Svalbard, *Tellus* 69B, 1311767, DOI: 10.1080/16000889.2017.1311767, 2017.
- Ishidoya, S., and Murayama, S.: Development of high precision continuous measuring system of the atmospheric O_2/N_2 and Ar/N_2 ratios and its application to the observation in Tsukuba, Japan, *Tellus* B, 66, 22574, <http://dx.doi.org/10.3402/tellusb.v66.22574>, 2014.
- Ishidoya, S., Tsuboi, K., Murayama, S., Matsueda, H., Aoki, N., Shimosaka, T., Kondo, H., and Saito, K.: Development of a continuous measurement system for atmospheric O_2/N_2 ratio using a paramagnetic analyzer and its application in Minamitorishima Island, Japan, *SOLA*, 13, 230–234, 2017.

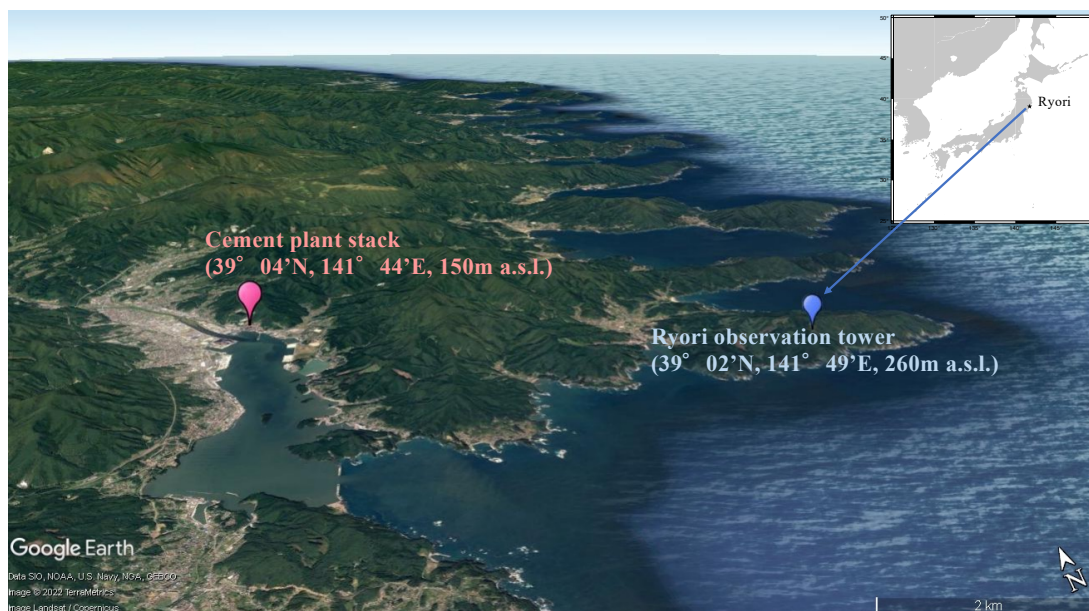


- Ishidoya, S., Sugawara, H., Terao, Y., Kaneyasu, N., Aoki, N., Tsuboi, K., and Kondo, H.: O₂ : CO₂ exchange ratio for net turbulent flux observed in an urban area of Tokyo, Japan, and its application to an evaluation of anthropogenic CO₂ emissions, *Atmos. Chem. Phys.*, 20, 5293–5308, <https://doi.org/10.5194/acp-20-5293-2020>, 2020.
- Ishidoya, S., Tsuboi, K., Niwa, Y., Matsueda, H., Murayama, S., Ishijima, K., and Saito, K.: Spatiotemporal variations of the $\delta(\text{O}_2/\text{N}_2)$, CO₂ and $\delta(\text{APO})$ in the troposphere over the western North Pacific, *Atmos. Chem. Phys.*, 22, 6953–6970, <https://doi.org/10.5194/acp-22-6953-2022>, 2022.
- Japan Cement Association: Handbook of Cement, 2020.
- Kannari, A., Tonooka, Y., Baba, T., Murano, K.: Development of multiple-species 1 km×1 km resolution hourly basis emissions inventory for Japan, *Atmos. Environ.*, 41, 3428–3439, 2007.
- 325 Keeling, R. F.: Development of an interferometric oxygen analyzer for precise measurement of the atmospheric O₂ mole fraction, *Ph.D. thesis*, Harvard University, Cambridge, 1988.
- Keeling, R. F. and Shertz, S. R. 1992. Seasonal and interannual variations in atmospheric oxygen and implications for the global carbon cycle, *Nature*, 358, 723-727.
- Keeling, R. F., Bender, M. L., and Tans, P. P.: What atmospheric oxygen measurements can tell us about the global carbon cycle, *Global Biogeochem. Cycles*, 7, 37-67, 1993.
- 335 Keeling, R. F., Manning, A. C., and Dubey, M. K.: The atmospheric signature of carbon capture and storage, *Phil. Trans. R. Soc. A*, 369, 2113-2132 doi: 10.1098/rsta.2011.0016, 2011.
- Kondo, H., Saigusa, N., Murayama, S., Yamamoto, S., and Kannari, A.: A numerical simulation of the daily variation of CO₂ in the central part of Japan—summer case—, *J. Meteor. Soc. Japan. Ser. II*, 79, 11-21, 2001.
- 340 Leeuwen, C.V., and Meijer, H.A.J.: Detection of CO₂ leaks from carbon capture and storage sites with combined atmospheric CO₂ and O₂ measurements, *Int. J. Greenh. Gas Control*, 41, 194–209, 2015.
- Manning, A. C. and Keeling, R. F.: Global oceanic and land biospheric carbon sinks from the Scripps atmospheric oxygen flask sampling network. *Tellus B*. 58, 95– 116, 2006.
- Minejima, C., Kubo, M., Tohjima, Y., Yamagishi, H., Koyama, Y., Maksyutov, S., Kita, K., and Mukai, H.: Analysis of $\Delta\text{O}_2/\Delta\text{CO}_2$ ratios for the pollution events observed at Hateruma Island, Japan, *Atmos. Chem. Phys.*, 12, 2713–2723, <https://doi.org/10.5194/acp-12-2713-2012>, 2012.
- 345 Nakazawa, T., Sugawara, S., Inoue, G., Machida, T., Makshutov, S. and Mukai, H.: Aircraft measurements of the concentrations of CO₂, CH₄, N₂O and CO and the carbon and oxygen isotopic ratios of CO₂ in the troposphere over Russia. *J. Geophys. Res.* 102, 3843– 3859, 1997.
- 350 Nara, H., Tanimoto, H., Nojiri, Y., Mukai, H., Zeng, J., Tohjima, Y., and Machida, T.: CO emissions from biomass burning in South-east Asia in the 2006 El Niño year: shipboard and AIRS satellite observations, *Environmental Chemistry* 8(2) 213-223 <https://doi.org/10.1071/EN10113>, 2011.
- Niwa, Y., Tsuboi, K., Matsueda, H., Sawa, Y., Machida, T., Nakamura, M., Kawasato, T., Saito, K., Takatsuji, S., Tsuji, K., Nishi, H., Dehara, K., Baba, Y., Kuboike, D., Iwatsubo, S., Ohmori, H., and Hanamiya, Y.: Seasonal Variations of CO₂,

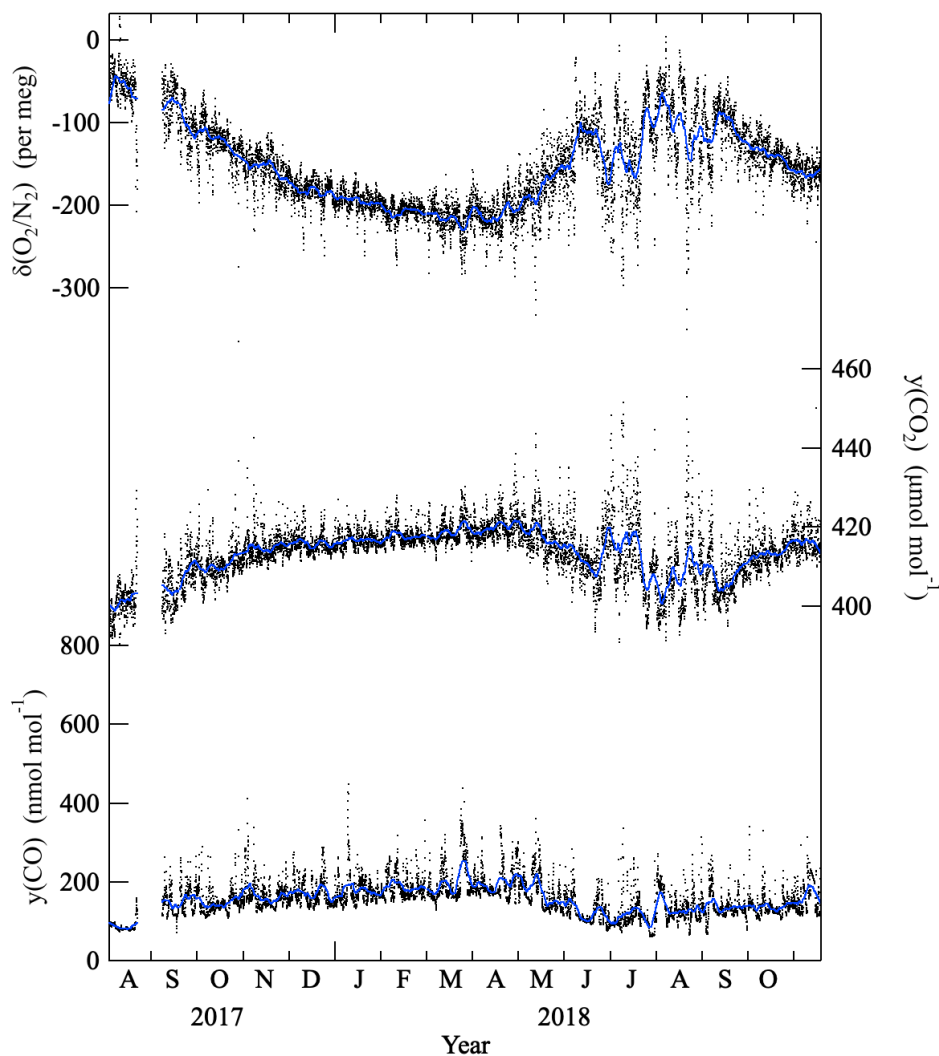


- 355 CH₄, N₂O and CO in the Mid-troposphere over the Western North Pacific Observed using a C-130H Cargo Air- craft, J. Meteorol. Soc. Japan, 92(1), doi:10.2151/jmsj.2014- 104, 2014.
- Pak, N. M., Rempillo, O., Norman, A-L., and & Layzell, D. B.: Early atmospheric detection of carbon dioxide from carbon capture and storage sites, J. Air Waste Manag. Assoc., 66, 739-747, doi: 10.1080/10962247.2016.1176084, 2016.
- 360 Resplandy, L., Keeling, R.F., Eddebbar, Y., Brooks, M., Wang, R., Bopp, L., Long, M. C., Dunne, J. P., Koeve, W., and Oschlies, A.: Quantification of ocean heat uptake from changes in atmospheric O₂ and CO₂ composition, Sci. Rep., 9, 20244, doi:10.1038/s41598-019-56490-z, 2019.
- Severinghaus, J.: Studies of the terrestrial O₂ and carbon cycles in sand dune gases and in biosphere 2, Ph. D. thesis, Columbia University, New York, 1995.
- Stephens, B. B., Keeling, R. F., Heimann, M., Six, K. D., Murnane, R., and Caldeira, K.: Testing global ocean carbon cycle 365 models using measurements of atmospheric O₂ and CO₂ concentration, Global Biogeochem. Cycles, 12, 213–230, 1998.
- Sugawara, H., Ishidoya, S., Terao, Y., Takane, Y., Kikegawa, Y., and Nakajima, K.: Anthropogenic CO₂ emissions changes in an urban area of Tokyo, Japan, due to the COVID-19 pandemic: A case study during the state of emergency in April– May 2020. Geophysical Research Letters, 48, e2021GL092600. https://doi. org/10.1029/2021GL092600, 2021.
- Tohjima, Y., Machida, T., Watai, T., Akama, I., Amari, T., and Moriwaki, Y.: Preparation of gravimetric standards for 370 measurements of atmospheric oxygen and reevaluation of atmospheric oxygen concentration, J. Geophys. Res., 110, D1130, 2005.
- Tohjima, Y., Kubo, M., Minejima, C., Mukai, H., Tanimoto, H., Ganshin, A., Maksyutov, S., Katsumata, K., Machida, T., and Kita, K.: Temporal changes in the emissions of CH₄ and CO from China estimated from CH₄ / CO₂ and CO / CO₂ correlations observed at Hateruma Island, Atmos. Chem. Phys., 14, 1663–1677, https://doi.org/10.5194/acp-14-1663- 375 2014, 2014.
- Tsuboi, K., Matsueda, H., Sawa, Y., Niwa, Y., Takahashi, M., Takatsuji, S., Kawasaki, T., Shimosaka, T., Watanabe, T., Kato, K.: Scale and stability of methane standard gas in JMA and comparison with MRI standard gas, Papers in Meteorology and Geophysics, Vol.66, 15-24, 2016.
- Wada, A., Matsueda, H., Sawa, Y., Tsuboi, K., and Okubo, S.: Seasonal variation of enhancement ratios of trace gases observed 380 over 10 years in the western North Pacific, Atmos. Environ., 45, 2129–2137, 2011.
- Yamagishi, H., Tohjima, Y., Mukai, H., and Sasaoka, K.: Detection of regional scale sea-to-air oxygen emission related to spring bloom near Japan by using in-situ measurements of the atmospheric oxygen/nitrogen ratio, Atmos. Chem. Phys., 8, 3325–3335, https://doi.org/10.5194/acp-8-3325-2008, 2008.

385



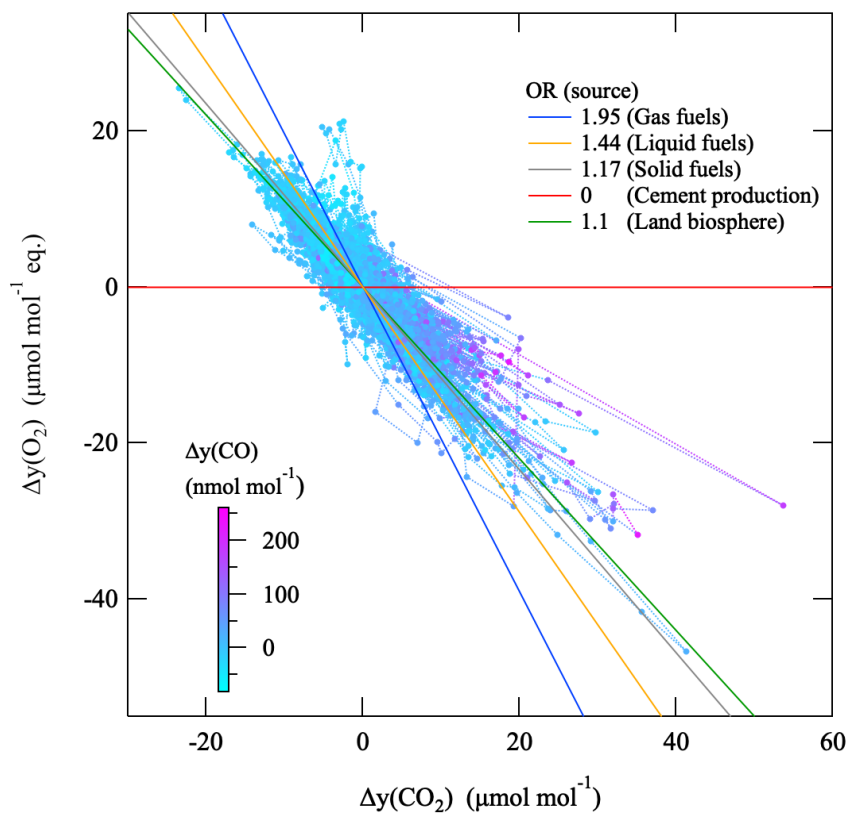
390 **Figure 1:** Location of the Ryori site (RYO) and the cement plant on an aerial photograph from © Google Earth. The cement plant is about 6 km northwest of RYO.



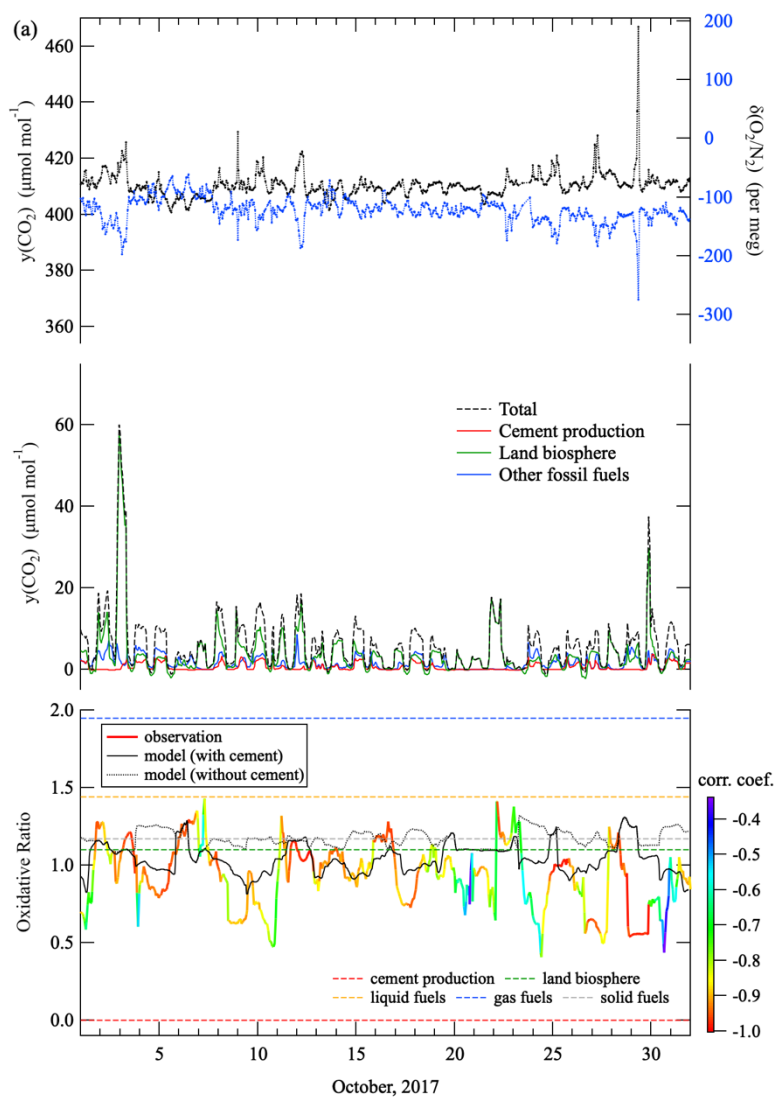
395

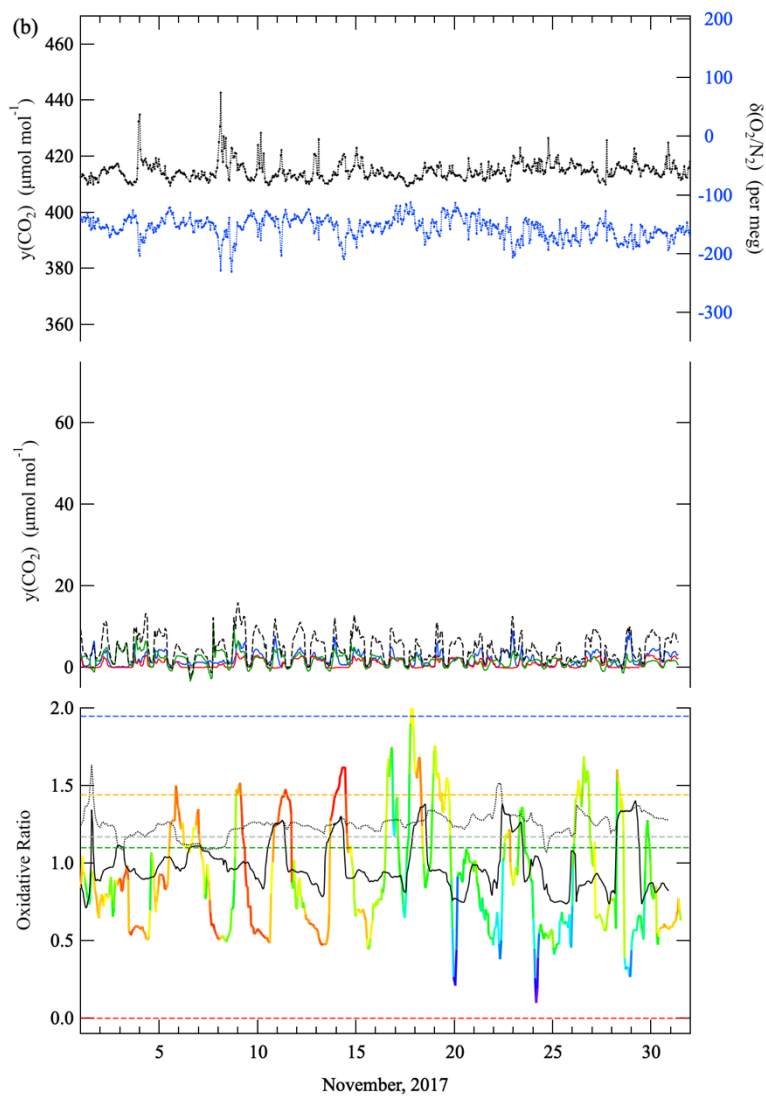
Figure 2: $\delta(\text{O}_2/\text{N}_2)$ and CO_2 and CO amount fractions (black dots) and their 1-week average values (blue lines) observed at Ryori (RYO), Japan, from August 2017 to November 2018.

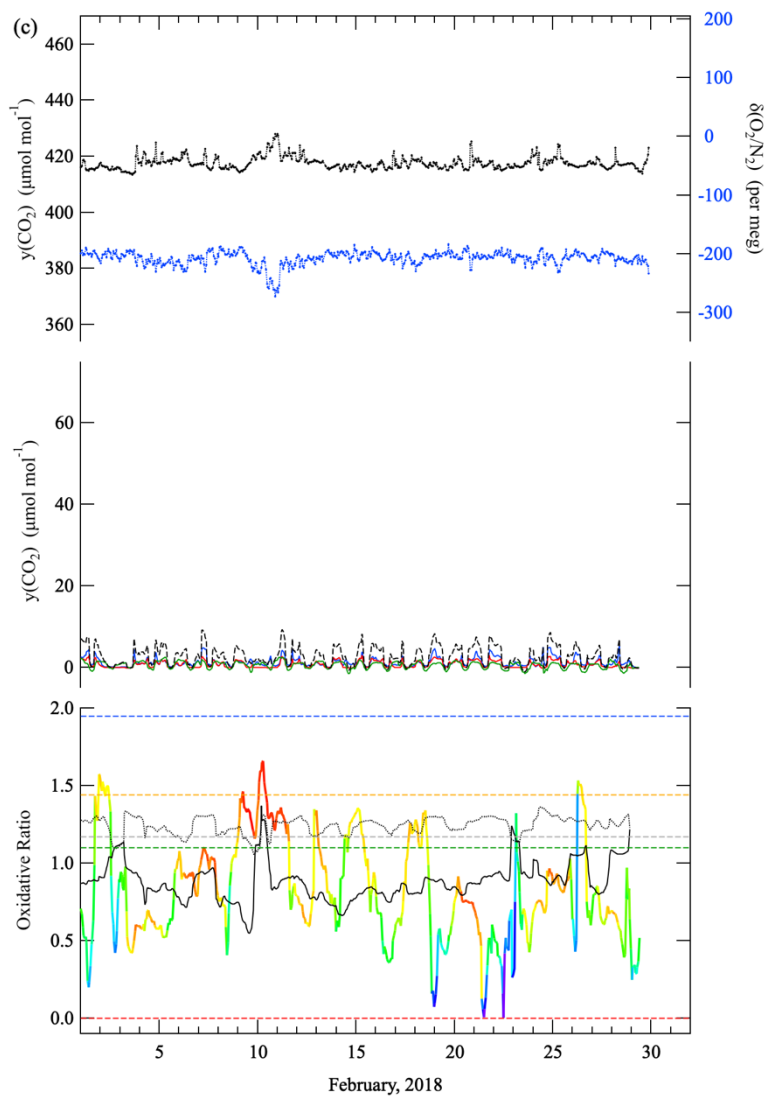
400

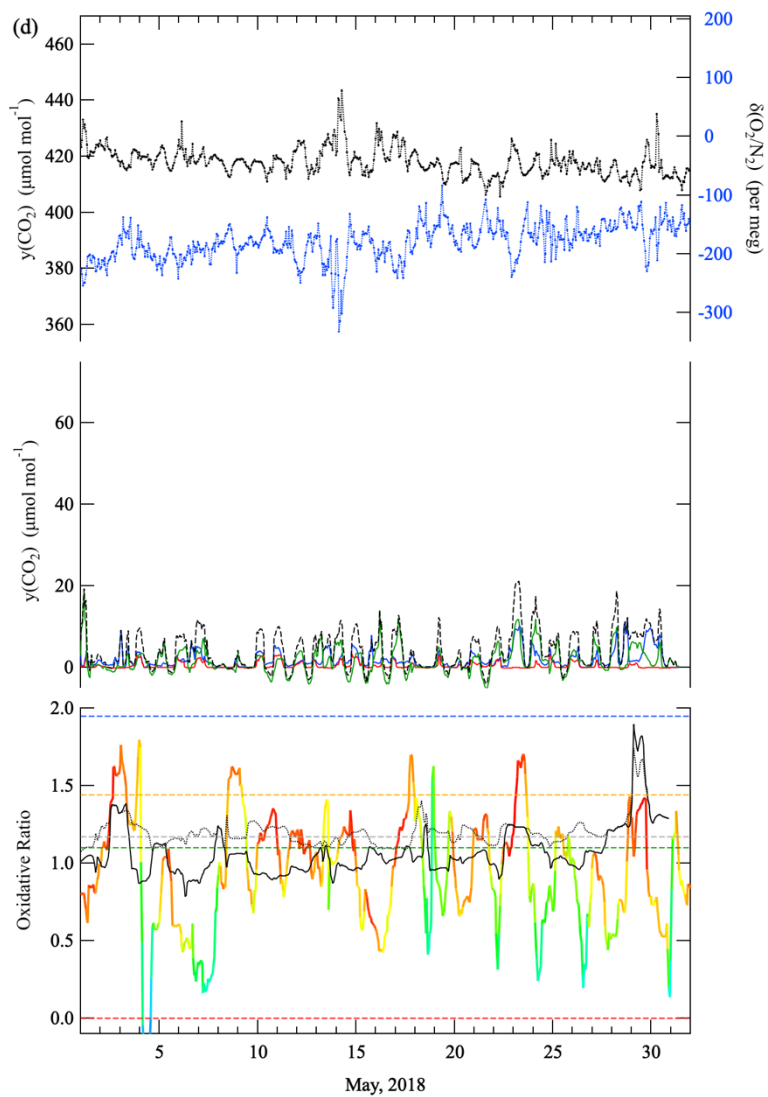


405 **Figure 3: Relationship between $\Delta y(\text{O}_2)$ and $\Delta y(\text{CO}_2)$ at RYO for the period from August 2017 to November 2018. $\Delta y(\text{O}_2)$, $\Delta y(\text{CO}_2)$, and $\Delta y(\text{CO})$ were calculated by subtracting the 1-week mean values of $\delta(\text{O}_2/\text{N}_2)$, CO_2 and CO amount fractions from their observed values; then $\Delta\delta(\text{O}_2/\text{N}_2)$ values were converted to the equivalent $\Delta y(\text{O}_2)$. $\Delta y(\text{CO})$ values are shown by the color scale. The plotted OR values are from Keeling (1988) and Severinghaus (1995).**



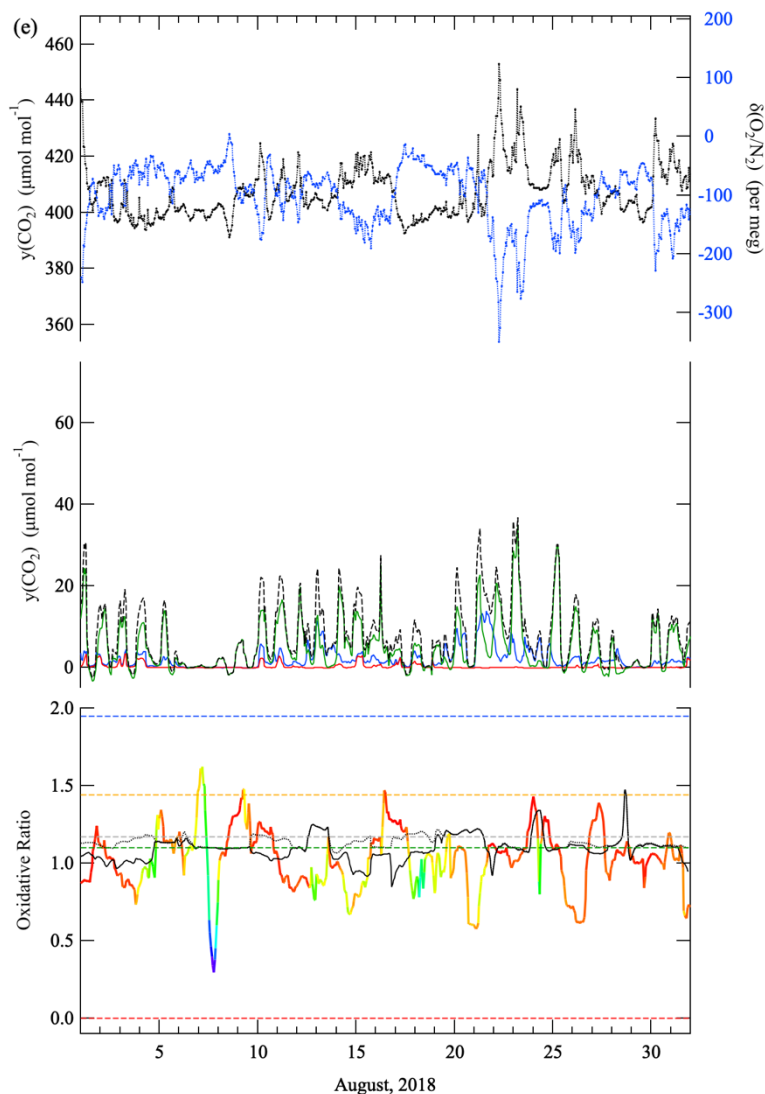








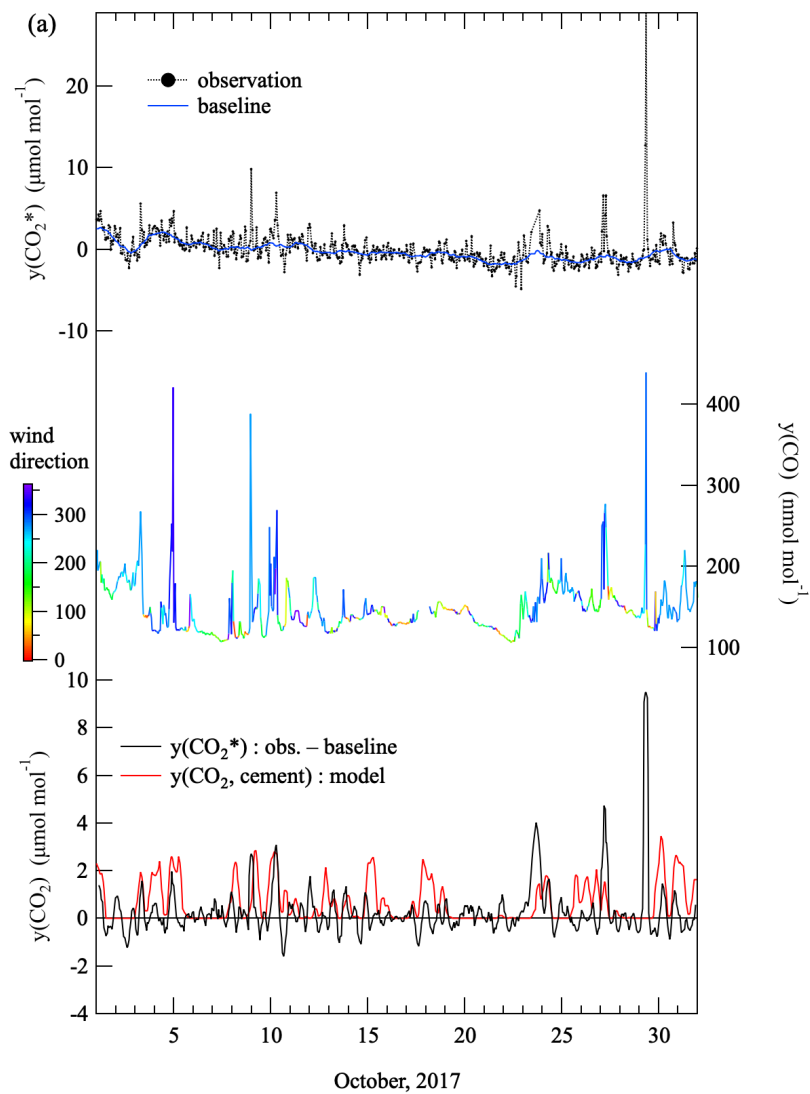
425

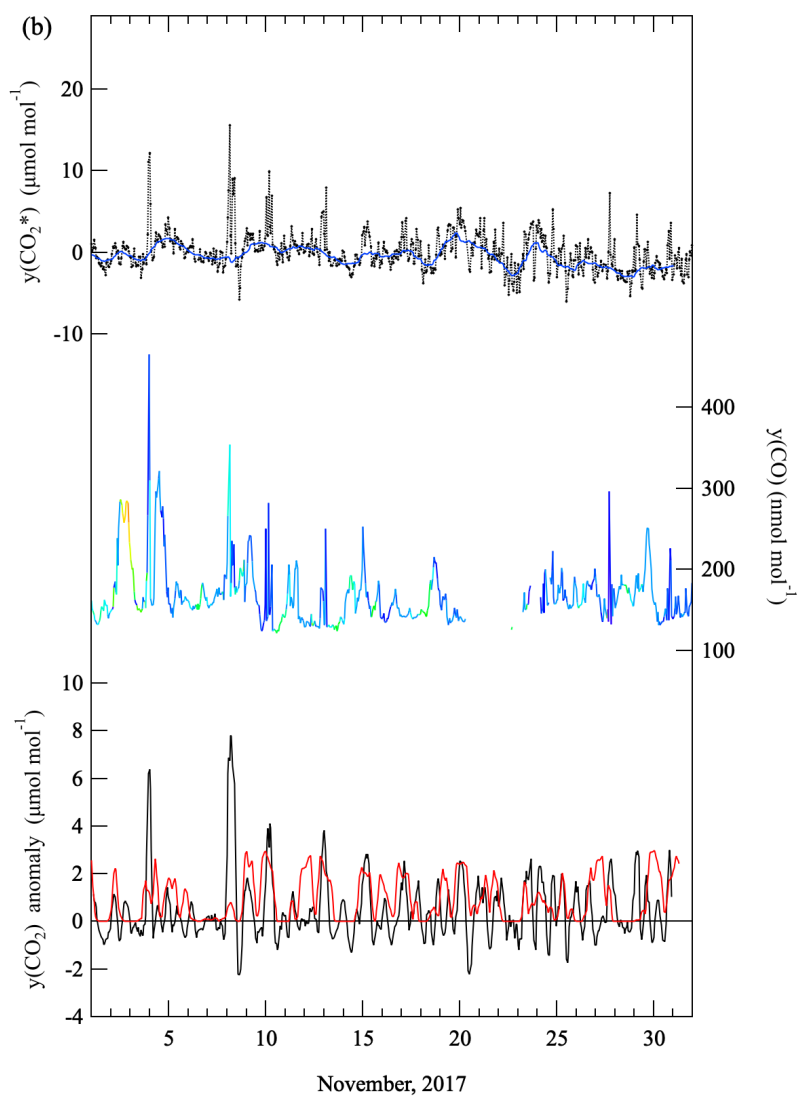


430

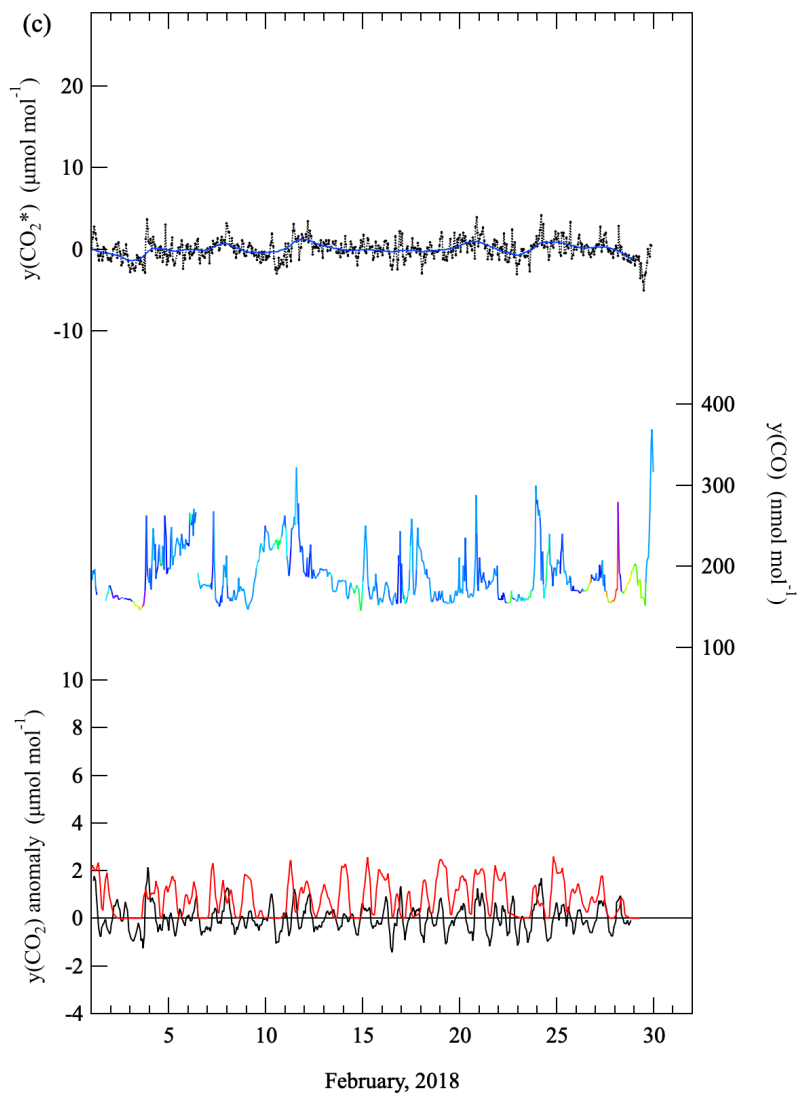
435

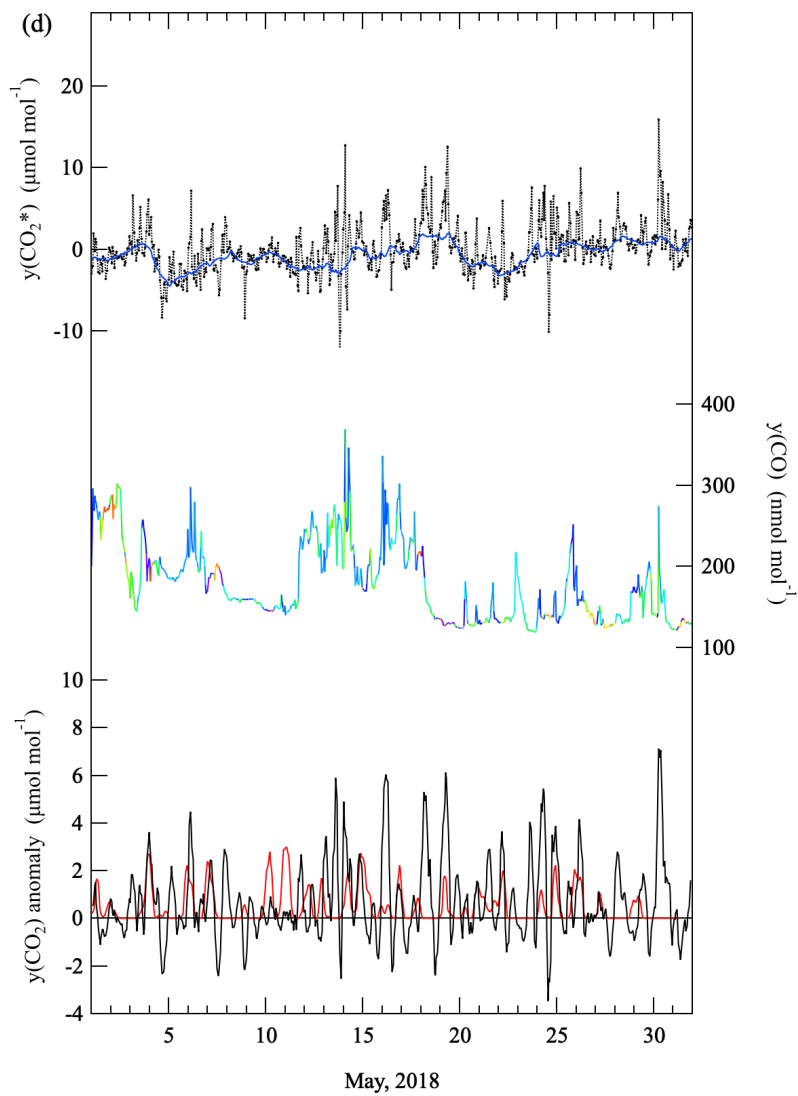
Figure 4: (a) (top) Variations in CO₂ amount fractions and $\delta(\text{O}_2/\text{N}_2)$ observed at RYO in October 2017. (middle) Variations in the total CO₂ amount fraction simulated by the AIST-MM (black dashed line, see text), and the contributions of CO₂ amount fraction for cement production (red solid line), terrestrial biospheric activities (green solid line), and fossil fuel consumption other than cement production (blue solid line). The simulated CO₂ amount fraction were calculated from the sources and sinks in East Japan area with no background amount fraction. (bottom) Variations in the oxidative ratio (OR) calculated by least-squares fitting of regression lines to the observed $\delta(\text{O}_2/\text{N}_2)$ and CO₂ values during successive 24-h periods (thick colored line, where the line color indicates the value of the correlation coefficient). The corresponding OR values calculated from the simulated O₂ and CO₂ amount fractions by the AIST-MM with and without considering the amount fraction of cement production are shown by black and gray solid lines, respectively. Dashed horizontal lines show the expected OR values for the consumption of gas, liquid, and solid fuels (Keeling, 1988); terrestrial biospheric activities (Severinghaus, 1995); and cement production. (b) As (a), but for November 2017. (c) As (a), but for February 2018. (d) As (a), but for May 2018. (e) As (a), but for August 2018.

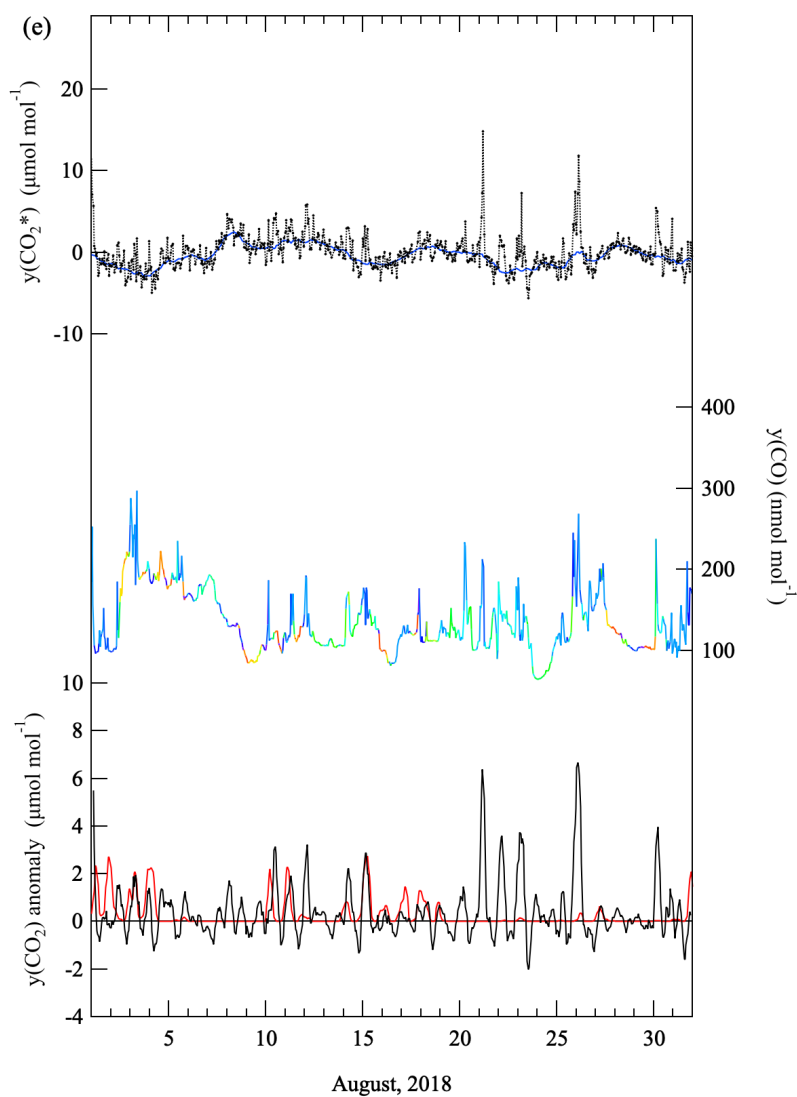




445



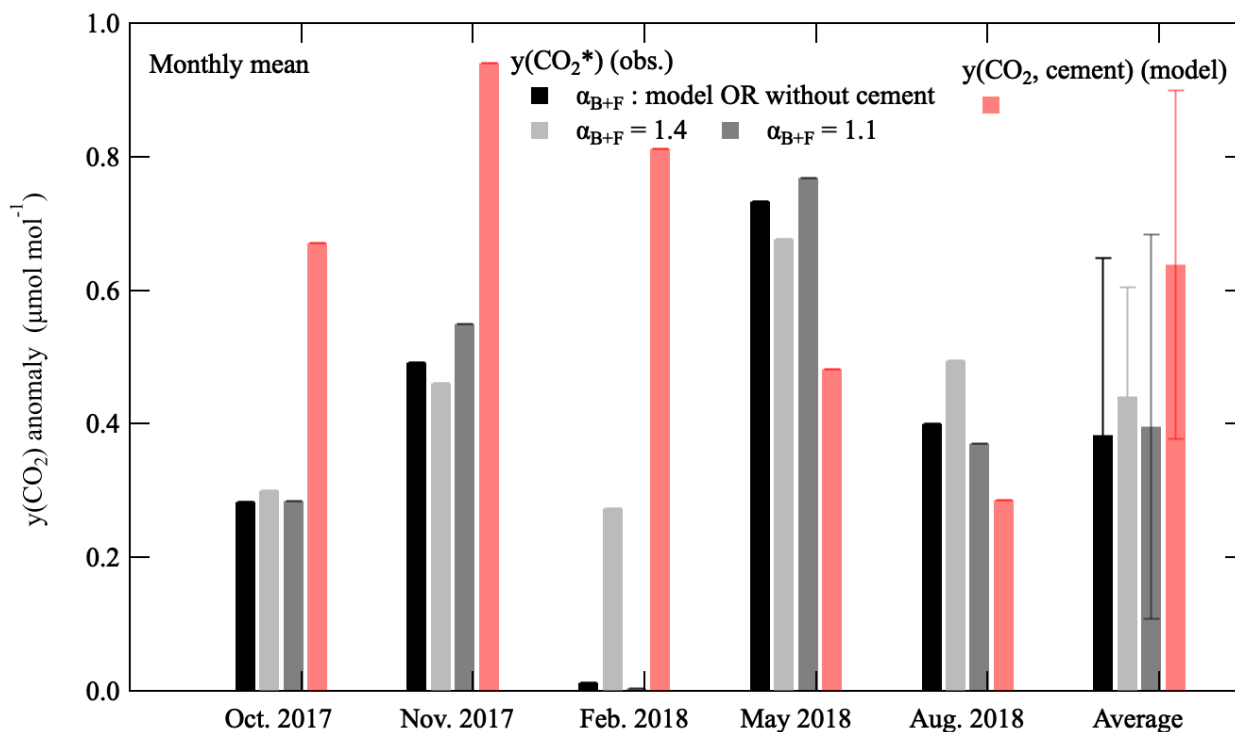




460

Figure 5: (a) (top) Variations in $y(\text{CO}_2^*)$ calculated from the observed CO_2 amount fractions and $\delta(\text{O}_2/\text{N}_2)$ (black filled circles) in October 2017, and the baseline variation (blue solid line). See text for the definition of $y(\text{CO}_2^*)$ and the method used to obtain the baseline variation. (middle) Variations in CO amount fractions in October 2017 and the simultaneously observed wind direction (in degrees). (bottom) Five-hour-average $y(\text{CO}_2^*)$ anomalies from the $y(\text{CO}_2^*)$ baseline variation and the corresponding variation in the CO_2 amount fraction due only to cement production ($y(\text{CO}_2, \text{cement})$) simulated by the AIST-MM (same as the red line in the middle part of Fig. 4a). (b) As (a), but for November 2017. (c) As (a), but for February 2018. (d) As (a), but for May 2018. (e) As (a), but for August 2018.

470



475 **Figure 6:** Monthly means of $y(\text{CO}_2^*)$ anomalies, obtained using model-simulated $\alpha_{\text{B+F}}$ values (as in Fig. 5a–e) and $\alpha_{\text{B+F}}$ values of 1.4 and 1.1, and $y(\text{CO}_2, \text{cement})$. The monthly mean values averaged over the 5 months are shown at the right. Error bars indicate monthly variability ($\pm 1 \sigma$).